Journal of Biomolecular Structure and Dynamics

ISSN: (Print) (Online) Journal homepage: https://www.tandfonline.com/loi/tbsd20

Three-dimensional modeling of streptomycin binding single-stranded DNA for aptamer-based biosensors, a molecular dynamics simulation approach

Masoumeh Nosrati & Mahmoud Roushani

To cite this article: Masoumeh Nosrati & Mahmoud Roushani (2022): Three-dimensional modeling of streptomycin binding single-stranded DNA for aptamer-based biosensors, a molecular dynamics simulation approach, Journal of Biomolecular Structure and Dynamics, DOI: 10.1080/07391102.2022.2050945

To link to this article: https://doi.org/10.1080/07391102.2022.2050945

JOURNAL OF BIOMOLECULAR STRUCTURE AND DYNAMICS
https://doi.org/10.1080/07391102.2022.2050945

Taylor & Francis
Taylor & Francis Group

Three-dimensional modeling of streptomycin binding single-stranded DNA for aptamer-based biosensors, a molecular dynamics simulation approach

Masoumeh Nosrati and Mahmoud Roushani

Department of Chemistry, Ilam University, Ilam, Iran

Communicated by Ramaswamy H. Sarma

ABSTRACT

Streptomycin (STR) an aminoglycoside antibiotic which is used against bacteria in human and animal infection, have serious side effects on different parts of human body. Therefore, there is a crucial need to detect trace amount of it in serum and food products. Aptamers are oligonucleotides or peptides, which bind their targets with high affinity and specificity. These properties make aptamers as suitable candidates for biosensing applications. A 79-mer ss-DNA aptamer was applied for the detection of small amount of STR in various aptasensors. But there is no structural information on the STR-binding aptamer and molecular details underlying the aptamer-STR binding remain unexplored. In this study we provided a 3D-structural model for 79-mer ss-DNA aptamer from the sequence. Using docking program and molecular dynamics (MD) simulation we predicted the binding pocket of ss-DNA aptamer. Our results show STR streptose ring is buried within the groove of DNA model and capped by non Watson-Crick bases. STR interacts with aptamer through forming stable hydrogen bonds. Our computational findings are in fair agreement with experimental results. With the atomic structural details, we gained new insight into the Apt-STR binding interaction that can help to further optimize aptamer efficiency in biosensing applications.

ARTICLE HISTORY
Received 11 October 2021
Accepted 3 March 2022

KEYWORDS
Biosensor; 3D structure prediction; molecular dynamics simulation; ss-DNA aptamer; streptomycin

Introduction

Streptomycin, an aminoglycoside antibiotic, is known to treat gram negative infections in human and veterinary through targeting the ribosomal RNA of bacteria (Aubin-Tam et al., 2011; Dua et al., 2011; Granja et al., 2009; Liu et al., 2009). The widespread use of streptomycin as antibacterial drug in human, animal, and as food additive in agricultural products, results in serious side effects on human health such as nephrotoxicity and ototoxicity (de Oliveira et al., 2009; Krieger, 2001; Wegener, 2003; Zhou et al., 2013). Thus, development of sensitive determination methods capable of detection the small amount of STR in different environments is in great demand in food safety control.

Aptamers are short single-stranded oligonucleotides or peptides, which are optimized to bind a variety of targets with high affinity and specificity (Blank & Blind, 2005; Bock et al., 1992; Ellington & Szostak, 1990). As biorecognition elements, aptamers provide advantages over antibodies due to their ease of synthesis, robustness, low cost, reusability and high chemical stability (Bunka & Stockley, 2006; Jayasena, 1999). Aptamers are identified trough an in vitro systematic evolution of ligands by exponential enrichment process (SELEX) to specifically bind a desired target (Robertson & Joyce, 1990; Winkler et al., 2002), the high specificity of aptamers as their key features to detect and quantify the trace amount of targets, has exploited them for the development of aptamer-based biosensors in the areas of food safety control and clinical diagnosis. Nowadays, peptide aptamers as antibody alternative are able to bind their biological targets with high affinity and selectivity. Recently macrocyclic β-sheet mimetic of ARC protein was designed to bind DNA major groove as a transcription factor protein in drug therapy (Stefanucci et al., 2015, 2021). There are several experimental techniques such as nuclear magnetic resonance (NMR) spectroscopy and crystallographic approaches, which have been used to reveal the details of interaction of aptamers and their aminoglycoside targets (Tereshko et al., 2003). Despite theaccurate and detailed information obtained from such techniques, they are expensive and difficult to use. Take to account this limitation, there are a few co-crystal structures of aptamer-–ligands available. Therefore, the binding pocket of aptamers and molecular details of their interactions with targets are unknown in most cases. However, it is crucial to understand the binding details in developing of aptamer-based biosensors. In recent years, there have been significant progresses in computational approaches to investigate the aptamer-target interactions (Ahmad et al., 2021; Chen et al., 2021). Among different computational methods, molecular dynamics simulation is a powerful tool to investigate the real time conformational and dynamics changes which occurred upon the binding process.

CONTACT Masoumeh Nosrati masoumeh.nosrati@gmail.com; Mahmoud Roushani m.roushani@ilam.ac.ir; mahmoudroushani@yahoo.com Department of Chemistry, Ilam University, Ilam, Iran.

Supplemental data for this article can be accessed online at http://dx.doi.org/10.1080/07391102.2022.2050945

DNA aptamers are known to be more stable than their RNA counterparts, which are made them suitable candidates for biomedical applications. But have the drawback of lacking the relevant DNA structure prediction tools in comparison with RNA. Regarding to this limitation, there are a few known DNA-ligand complex structures. In this study using a coarse grained modeling software, we predicted the 3D structure of streptomycin specific 79-mer ss-DNA aptamer from the sequence. The 79-mer ss-DNA aptamer has been synthesized and identified by Zhou and coworkers (Zhou et al., 2013). Several experimental studies have shown 79-mer ss-DNA aptamer successfully binds STR with high affinity and specificity (Emrani et al., 2016; Ghanbari & Roushani, 2018; Roushani et al., 2018; Taghdisi et al., 2016; Yin et al., 2016a, 2016b, 2017; Zhao et al., 2017). In a study conducted by Zhou et al, they found nucleotide motifs of 79 mer ss-DNA which are predicted to be involved in binding STR (Zhou et al., 2013). These motifs posses guanine rich sequences that are mainly located at the loop parts of the aptamer based on Mfold prediction.

The stability of the aptamer- ligand complex is a principal factor of their applicability in the field of drug and medicine. The complex stability is governed by the type of interactions occurred between aptamer and ligand. The molecular details of such interactions are considered by computational techniques. Molecular dynamics simulation is used to investigate the interaction between aptamer and ligands at the atomic details. This information can help to optimize aptamer biosensing characteristics and plays a key role in reducing the number of experiments to design more target-specific aptasensors. The MD simulations provide invaluable and crucial information that is difficult to obtain experimentally. Using MD simulation, binding specificity, stability and conformational changes can be investigated. In the present study, using molecular docking and molecular dynamics simulation, we predicted the binding pocket of STR- specific aptamer along with structural details of aptamer-STR interactions. To our knowledge this is the first in silico study that predicts the 3D structural model of 79-mer ss-DNA aptamer and illustrates the Apt-STR binding characteristics.

Methods

Three-dimensional structure preparation

Due to the absence of experimentally 3D structure of 79-mer ss-DNA, we need to build the structure. First, the secondary structure of aptamer was predicted by Mfold software which gives typical loop and stem motifs (Zuker, 2003). Based on Mfold secondary structure, the 3D model of the aptamer was generated with MacroMolecularBuilder (MMB) (Flores et al., 2011), a coarse-grained modeling software. The Autodock docking program (Autodock vina) (Trott & Olson, 2010) was applied to dock ligand into the designed 3D aptamer structure (Figure 1). The best docking complex configuration was selected regarding to the residues involved (Zhou et al., 2013) and binding energy scores for subsequent MD simulation. The geometry optimization of streptomycin was performed with RHF/6-31G* basis set using *Gaussian09* (Frisch et al., 2009).

Molecular dynamics simulation

The 3D aptamer and docked complex structures were employed as an input for all atom MD simulations. Aptamer and aptamer-STR complex were treated in two independent simulations.

The MD simulations were carried out with GROMACS software package version 5.1.1 (Hess et al., 2008) with the Amber 99SB force field (Case et al., 2005). The Amber force field has been used widely for nucleic acid studies. A TIP-3P water model and at least 47000 water molecules were used to solvate the structures in a dodecahedron box with a minimum distance of 10 Å between the aptamer and the box walls. Periodic boundary conditions were assigned to all directions. Adding sodium ions neutralized the net charge of the systems. The system energy was minimized employing steepest descent algorithm. The minimized structures were further equilibrated for 100 ps using NVT and NPT thermodynamic state ensembles, the temperature and pressure were constant at 300 K and 1 bar using Berendsen weak coupling method with coupling times of 0.1 and 2.0 ps, respectively (Berendsen et al., 1984). The particle mesh Ewald method was used for the electrostatic interaction (Darden et al., 1993). The LINCS algorithm was applied to constrain bond lengths (Hess et al., 1997). Dispersive interactions were used a Lennard-Jones potential with a 1 nm cutoff. Electrostatic interactions with a cut-off of 1.2 nm were considered. The streptomycin (STR) molecule has been integrated in to the simulation box. General Amber force field (GAFF) parameters were applied to the STR ligand by using Antechamber suite set in Amber Tools 20 package (Case et al., 2020). ACEPYPE was employed to transfer the resulting parameters to Gromacs compatible format (Da Silva & Vranken, 2012). The final MD simulations were conducted for 100 ns. The VMD (Visual Molecular Dynamics) software was used to visualize the MD simulation results (Humphrey et al., 1996).

Results and discussion

Simulation of the unstructured aptamer-streptomycin complex

In a research conducted by Zhou et al, they have reported a 79-mer ss-DNA aptamer that binds streptomycin with high specificity and affinity (Zhou et al., 2013). Through sequence analysis and affinity measurement, they found there are nucleotide motifs in 79-mer ss-DNA aptamer sequence, which are expected to be involved in STR binding. Based on Mfold secondary structure predictions, these motifs are located at the loop part of the ss-DNA aptamer and include motifs GGGG residues 23–26, GGTGTT residues 30–35 and GGGT residues 51–54.

In the first step of this in silico study and with the aim of finding the aptamer binding motifs, 30 ns MD simulation of

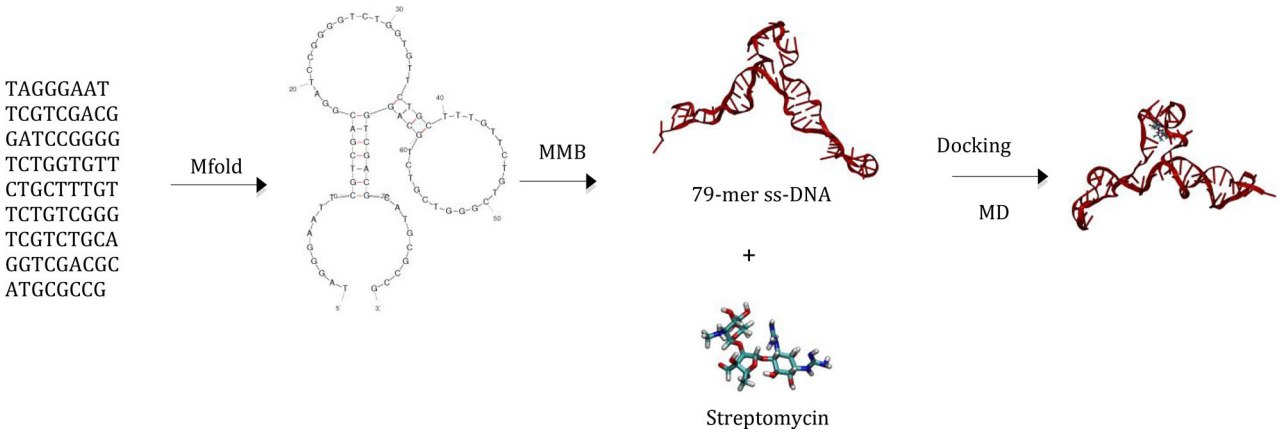

Figure 1. Schematic overview of workflow used to construct the 3 D structure of aptamer- streptomycin complex.

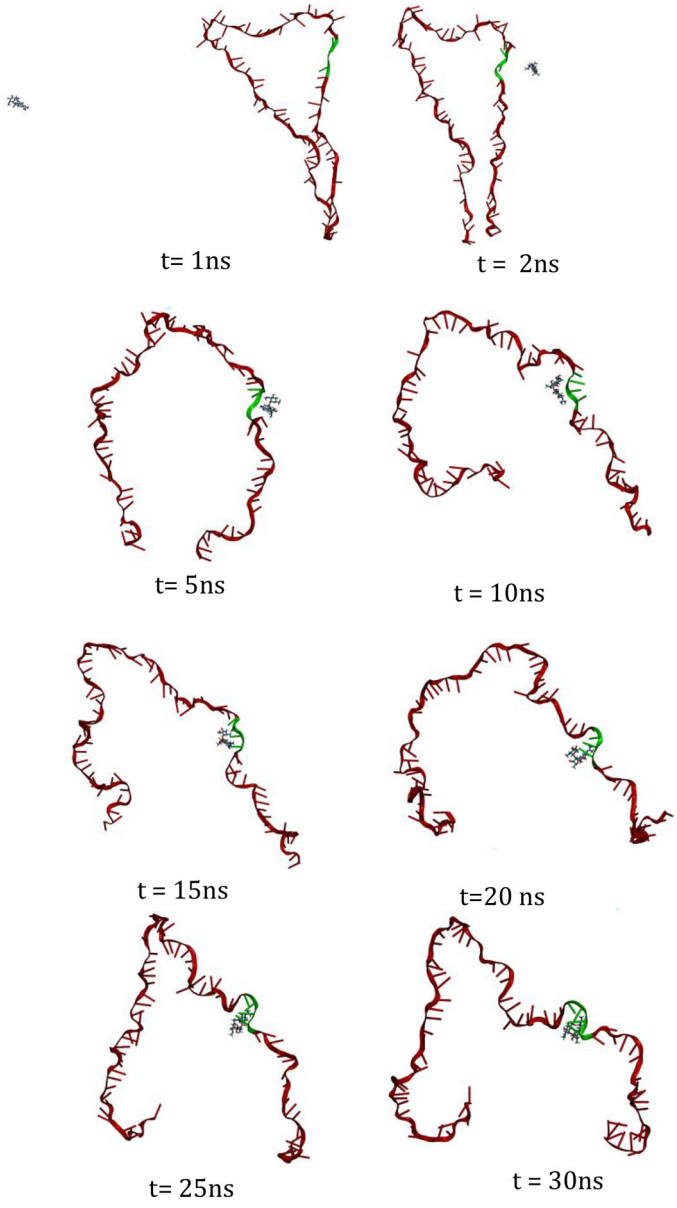

Figure 2. Combination evolution of unfolded ss-DNA aptamer and STR during 30 ns simulation time.

unfolded ss-DNA aptamer with STR was carried out. According to 30 ns MD simulation, STR chose the GGGG motif residues 23–26 of unfolded aptamer as illustrated in Figure 2. These residues are interacting with STR mostly through forming stable hydrogen bonds (Figure 3). Indeed 30 ns MD simulation indicates the key role of aptamer GGGG motif (residues 23–26) in binding process. These obtained results along with experimental data (Zhou et al., 2013) helped us to have an estimation of aptamer binding pocket in the subsequent docking calculation.

Simulation of the folded aptamer with and without bound streptomycin

In the next step, based on the secondary structure obtained from Mfold, the three dimensional model of 79-mer ss-DNA was generated using MMB coarse-grained software. With the aim of finding the suitable binding mode of ss-DNA aptamer and streptomycin, docking calculation was performed. The best complex was selected according to the residues involved and binding energy score. We used this final complex as an input for MD simulation. The results of 30 ns MD simulation and docking calculation showed the motif GGGG residues 23–26 along with motif GGTGTT residues 30–35 are important parts of the apatmer-binding pocket. In the next step, two 100 ns MD simulation of folded aptamer (generated by MMB) without and with STR (obtained from docking simulation) were carried out. The Apt-STR complex simulation show STR trapped inside a binding pocket constituted by residues 18–35, which includes two nucleotide motifs 23–26 and 30–35, these motifs predicted to be important in STR binding based on Zhou et al studies (Figure 4). We compared 79-mer ss-DNA binding pocket with that of streptomycin specific 40-mer RNA aptamer obtained from Tereshko et al crystallographic studies (Tereshko et al., 2003) similar to 40-mer RNA binding pocket, in ss-DNA aptamer, STR streptose ring is buried inside the deep groove of DNA and capped by non Watson-Crick bases including G25–G31 and G24–T32 pairs (Figure 4).

Structural stability of the aptamer

To investigate the aptamer structural stability during the MD simulation, the root mean square deviations (RMSD) analysis of aptamer backbone was applied; the reference structure was energy-minimized structure in all simulations. As

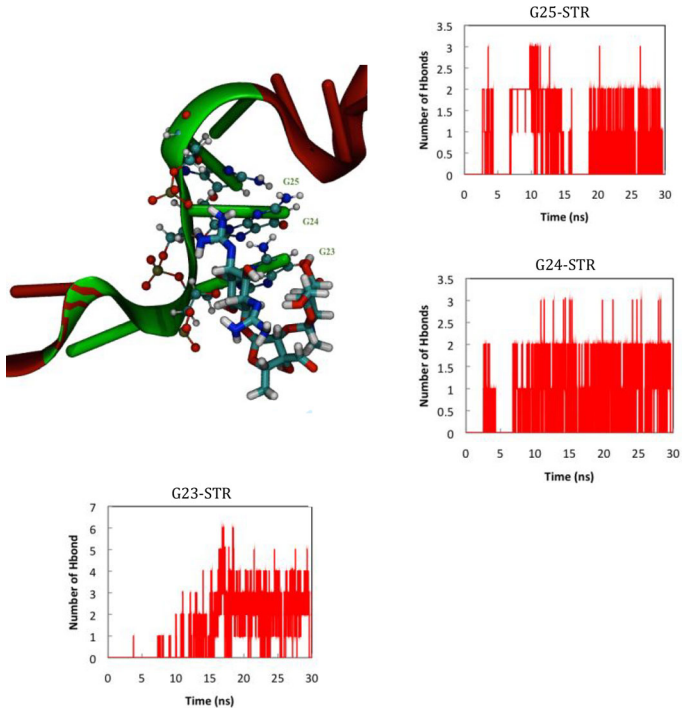

Figure 3. STR hydrogen bond interactions with G23-25 motif of unfolded ss-DNA aptamer.

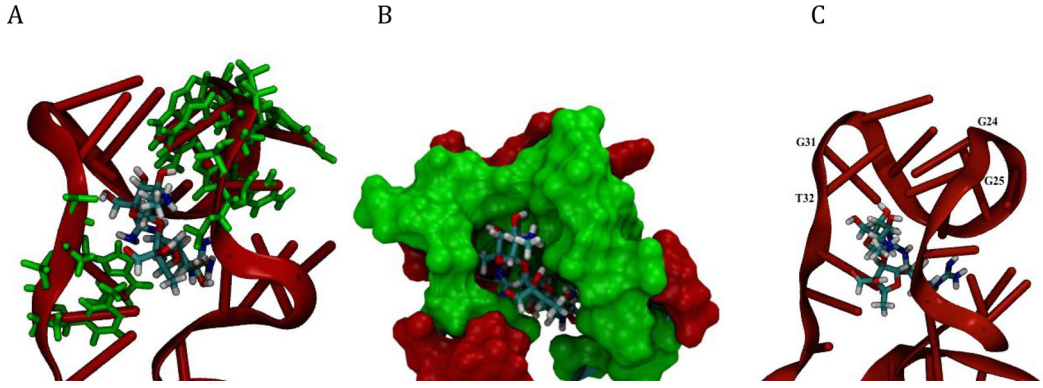

Figure 4. Average conformation of binding pocket region in interaction with bound STR (A) The aptamer involved residues shown in green sticks are interacting with STR (B) Schematic illustration of STR trapping in a deep groove of DNA cavity, the interacting residues with STR are presented by green color (C) STR capped by non Watson-Crick bases including G25–G31 and G24–T32.

displayed in Figure S1, unfolded bound-aptamer structure shows the highest RMSD values. The folded bound aptamer structure after ~20 ns of simulation time becomes stable, comparison of bound and unbound aptamer RMSD plots in the folded state, indicates in the presence of ligand, aptamer large fluctuations are considerably reduced, demonstrative of occurring significant interactions between aptamer and STR. We calculated the RMSD of the binding pocket region including residues 18–35, as Figure S1 shows, after ~20 ns of simulation time, RMSD fluctuations become stable around 0.18 nm in complex structure, indicating that the binding pocket structure is unperturbed during the simulation time. From the RMSD plot of binding pocket region, it is clear that the motile nature of DNA aptamer is considerably reduced upon complex formation. STR rigidifies the binding pocket due to the stable formed hydrogen bonds with aptamer.

The root-mean-square fluctuations (RMSF) analysis was performed to evaluate the aptamer flexibility changes that occurred upon interactions with STR during 100 ns MD simulation. The RMSF values for aptamer in both unbound and bound states are displayed in Figure S2. As it can be seen from this figure, the large fluctuations of key residues located at the binding pocket region have decreased significantly upon complex formation (residues 18–35) demonstrative of stable combination of DNA aptamer with STR. The binding pocket region in unbound structure shows high fluctuations indicating the more residue freedom and dynamics in the absence of STR. The highest fluctuations were observed for residues 19, 20, 26 and 30 in both bound and unbound states, by inspecting the complex structure we found these residues are not participated in hydrogen bond interactions with STR.

Radius of gyration

Radius of gyration (Rg) is a measure of aptamer compactness and stability in the process of molecular dynamics simulation. The Rg values for aptamer in both bound and unbound

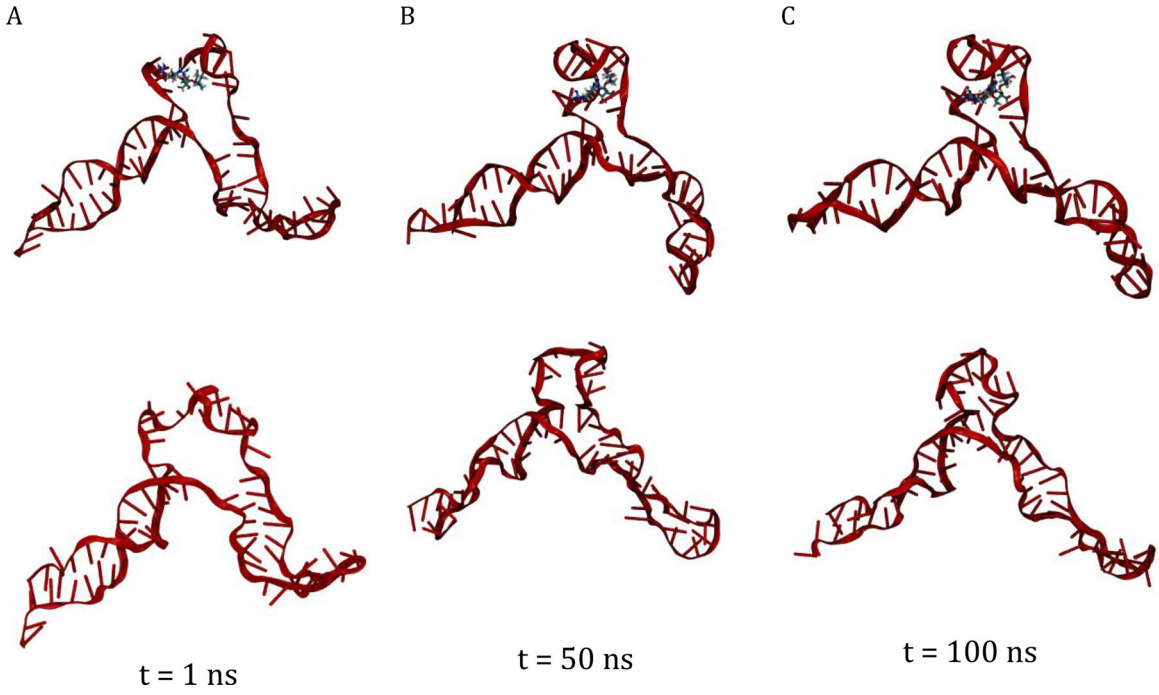

Figure 5. MD snapshots of aptamer in bound and unbound states at time intervals of 50 ns.

Table 1. Hydrogen bond characteristics of involved residues in Hbond interaction[a].

Don	Acc	Dist (Å)	Don	Acc	Dist (Å)
STR:N1	G18:OP1	1.81	G24:N1	STR:O44	2.18
STR:N1	G18:O5	2.82	G24:N2	STR:O44	2.41
STR:N4	G18:O5	3.13	STR:N3	C28:OP1	1.91
A19:N6	STR:O51	1.94	STR:N4	C28:OP1	2.12
STR:O53	A19:N7	2.14	STR:N19	C28:O2	1.85
STR:O51	C21:O2	2.92	G31:N1	STR:O42	3.17
STR:O53	C21:O2	2.80	G31:N1	STR:N19	2.54
STR:O30	C22:OP2	1.80	G31:N2	STR:N19	3.35
STR:N48	C22:OP2	1.96	STR:O42	T32:O2	3.25
STR:O46	G23:O6	3.34	STR:O44	T32:O2	1.85
STR:O46	G23:N7	2.11	STR:N18	G33:N7	3.47
G24:N1	STR:O46	2.81	STR:O42	G33:OP2	1.97

[a]Abbreviations: Don; Donor groups, Acc; Acceptor groups and Dist; Distance in Angstroms.

states were plotted and compared to each other. As Figure S3 shows, the Rg values of binding pocket region in the bound state were reduced considerably and fluctuations were negligible. As illustrated in Figure S3, Rg converged to 0.9 nm after nearly 20 ns and remained stable during the simulation time. This demonstrates the consistency of lignad binding and stability of Apt-STR complex. Thus, the complex radius of gyration further validated the stable combination between aptamer and STR (Figure 5).

Surface accessible solvent area

Surface accessible solvent area (SASA) is defined as the surface area of DNA, which interacts with solvent. Average SASA of aptamer binding pocket region in bound and unbound states were monitored during 100 ns MD simulation. We calculated the SASA values per binding pocket residue in the unbound and bound states. The calculation shows, all binding pocket residues in complex structure have smaller SASA values comparing to corresponding residues in unbound structure (Table S1), which indicates these residues are involved in binding STR and their solvent exposure is reduced upon complex formation.

Hydrogen bond analysis

The recognition specificity of 79mer ss-DNA aptamer is associated with stable hydrogen bonds it made with STR. Hydrogen bonds play a key role in aptamer–ligand complex formation and stabilization. Tereshko et al have resolved the crystallographic structure of 40-mer RNA aptamer with STR (Tereshko et al., 2003), molecular dynamic simulations have been carried out to investigate the streptomycin interaction with this 40-mer RNA aptamer (Baptista & Netz, 2019; Nick et al., 2016), the results showed that streptomycin stabilized the RNA aptamer through forming stable hydrogen bonds.

In order to get further insight into the DNA-STR binding, the hydrogen bond analysis was carried out. According to gromacs, we considered hydrogen bonds with a maximum distance of 0.35 nm and 30° or less of corresponding angles between the donor and acceptors atoms. The hydrogen bond plots between binding pocket residues and STR indicated DNA combined with STR mostly through forming stable hydrogen bonds. Hydrogen bonds are occurred between binding pocket residues including C21, C22, G23, G24, G28, G31, T32, and G33 with STR as displayed in Figure 6 and Table 2. G25 shows occasional formed hydrogen bonds with STR. As illustrated in hydrogen bond graphs, it is obvious that all involved residues form several stable hydrogen bonds with STR, consistency and intensity of hydrogen bonds are clear from the depicted plots (Figure 7). The stability of hydrogen bonds was evaluated by plotting the distance values versus simulation time. The depicted plots show the consistent behaviors of hydrogen bonds throughout the

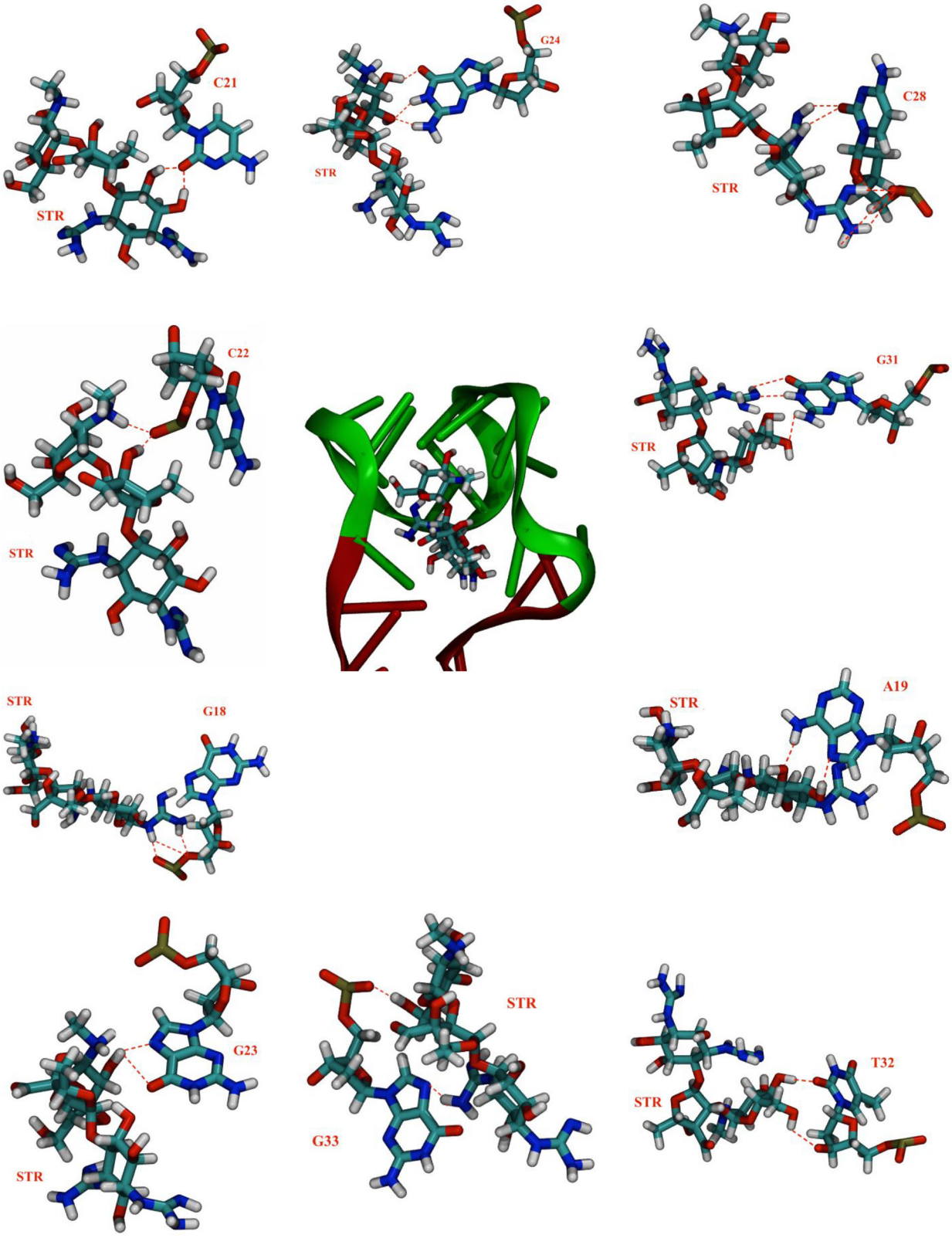

Figure 6. Average structure of Apt-STR complex. The hydrogen bond interactions between STR and Apt residues located at the binding pocket region are presented.

simulation time. The hydrogen bond distance values are reported in Table 2. The consistency and stability of hydrogen bonds are in good accordance with RMSD, Rg and RMSF data, as we described above RMSD values were reduced considerably in the binding pocket region indicating that high stability gained upon complex formation. The RMSF value reduction is indicative of involvement of residues in strong hydrogen bond interaction, as we can see in Figure S2, residues 19, 20, 26, and 30 have the highest RMSF values compared to other neighbor residues in the binding pocket region, these four residues are not involved in hydrogen bond interaction with STR. The average number of hydrogen

bonds between binding pocket residues and STR was calculated and plotted versus time in Figure 7(K). As graph shows after 20 ns of simulation time the plateau is occurred with average number of 14 hydrogen bonds. This is in good agreement with the number of hydrogen bonds reported in Tereshko et al crystallographic complex structure (Tereshko et al., 2003).

Binding energy

The binding energy of Apt-STR complex was evaluated using MM-PBSA to estimate the binding affinity of aptamer to ligand (Kumari et al., 2014). Our calculation shows aptamer bound streptomycin with binding energy of −43.943 kJ/mol. The contribution of different energy terms is reported in the Table 2. As data shows, the electrostatic energy term made the biggest contribution to the binding energy. This result demonstrated that electrostatic energy through forming stable hydrogen bonds plays an important role in aptamer- STR complex formation.

Table 2. Binding free energy obtained from MM-PBSA calculation.

Binding energy components (kJ/mol)	
ΔE_{vdw}	−196.294 ± 30.076
ΔE_{ele}	−706.394 ± 2.169
ΔG_{polar}	882.130 ± 8.967
$\Delta G_{nonpolar}$	−23.385 ± 1.007
ΔG_{bind}	−43.943 ± 38.517

All atom molecular dynamics simulation has made this possibility to consider the binding mechanism of STR and ss-DNA aptamer in atomic details. The base-to-base distances were calculated to investigate the binding mechanism. The separating distances between COM of T20–G33 and G22–G33 bases in the binding pocket region reduced upon complex formation from ∼2.7 to 1.7 nm and from 2.4 to 1.4 nm, respectively and remained stable during the 100 ns MD simulation time (Figure 8). Therefore ss-DNA aptamer conformation has changed upon STR binding, this demonstrates that aptamer-STR binding process corresponds to induced-fit mechanism. Our computational study show binding pocket region is separated from the two other parts of the aptamer and it is the only section of aptamer, which is involved in STR binding process. Moreover, several studies have revealed that there are many advantages of truncated aptamers such as cost effectiveness, easy management and higher specificity and affinity (Alhadrami et al., 2017; Kaur & Yung, 2012; Keefe et al., 2010; Le et al., 2014; Sussman et al., 2000). Hence, we suggest truncating 79 mer ss-DNA aptamer into shorter 34-mer DNA with conserved binding motifs, the secondary structure of truncated sequence was obtained from Mfold, as illustrated in the Figure 9, the truncated aptamer includes binding motifs GGGG and GGTGTT in one loop. We suggest this 34-mer aptamer for further STR-binding evaluation.

View of relative location of base pairs T20-G33 and C22-G33 in (C, D) free and (E,F) complex aptamer structures.

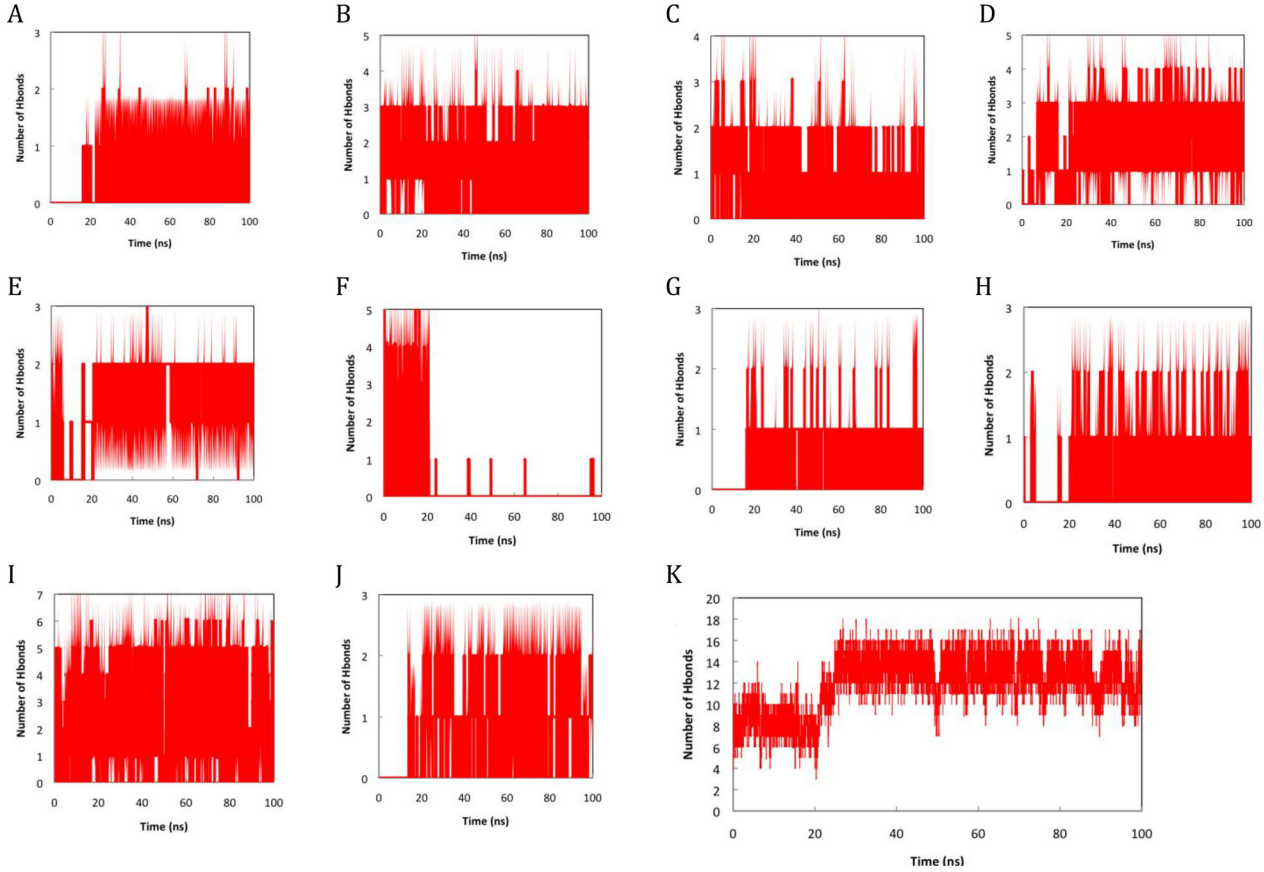

Figure 7. Hydrogen bond plots calculated between STR and binding pocket residues (A) G18 (B) A19 (C) C21 (D) C22 (E) G23 (F) G24 (G) G25 (H) G31 (I) T32 (J) G33 (K) Total Hbonds between STR and aptamer binding region.

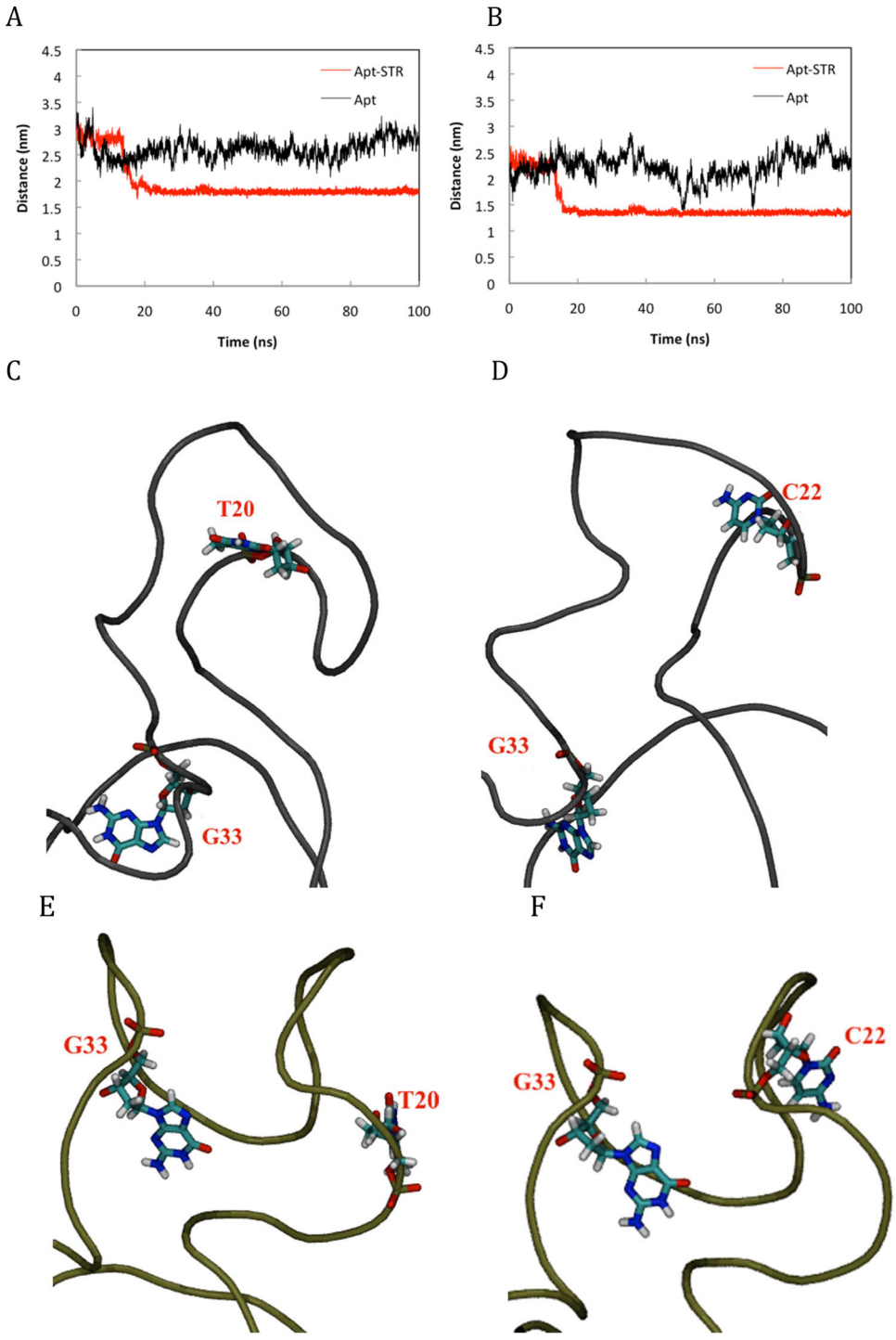

Figure 8. Calculated distances between residues (A) T20–G33 and (B) C22–G33 in binding pocket region.

Conclusion

Molecular dynamics simulation as a standard tool has expanded significantly in recent years to illustrate the bimolecular interactions in full atomic details. MD simulation can be used to elucidate the structural features of aptamers toward their targets and facilitate more efficient aptamer design for their therapeutic and diagnostic applications. MD simulation with real time analysis provides a detailed description of aptamer conformational dynamics to display an atomic illustration of binding process.

Using molecular modeling programs, including structural modeling, molecular docking and molecular dynamics simulation, we studied the binding characteristics of the 79-mer ss-DNA aptamer and streptomycin. In the present study, a 3D structural model of 79-mer ss-DNA aptamer was constructed and docked into STR. All-atom molecular dynamics simulations of ss-DNA aptamer without and with STR were carried out to investigate the binding process. Our docking and MD results show nucleotides 18–35 form a binding pocket region andthe residues 18, 19, 21, 22, 23, 24, 28, 31,

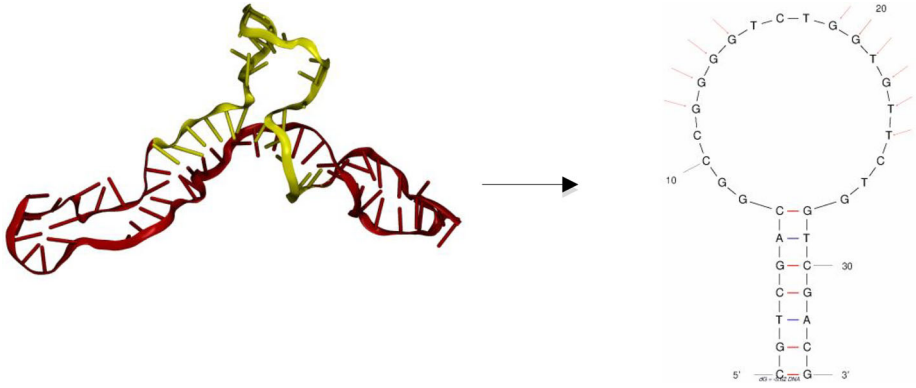

Figure 9. The secondary structure of truncated aptamer, generated by Mfold software. The 79-mer ss-DNA aptamer was truncated to new 34-mer aptamer, the truncated part including binding pocket region is shown in yellow. Truncated aptamer includes GGGG and GGTGTT motifs in one loop.

32 and 33 interact with STR through forming stable hydrogen bonds. Complex structure shows stabilization after ~20 ns of simulation time. The considerable reduction in RMSD, RMSF, Rg and SASA values, further validates the stable combination between aptamer and STR. In a research conducted by Zhou et al, through sequence analysis they found nucleotide motifs that appeared to be involved in STR binding. The computational results are in good accordance with their experimental findings, since our study shows those motifs are important parts of the binding pocket and are involved in hydrogen bond interactions with STR. The predicted binding pocket of ss-DNA, also shows meaningful similarity with that of streptomycin specific 40-mer RNA aptamer, obtained from crystallographic studies. By calculating the base to base distances in the binding pocket region, it concludes that Apt-STR interaction model corresponds to induced-fit binding mechanism. The results obtained from this in silico study lay the foundation for further optimized design of aptamers in biosensing applications.

Disclosure statement

No potential conflict of interest was reported by the authors.

Funding

This study financial support was provided by Ilam University.

ORCID

Masoumeh Nosrati http://orcid.org/0000-0001-8652-4988

References

Ahmad, N. A., Zulkifli, R. M., Hussin, H., & Nadri, M. H. (2021). In silico approach for Post-SELEX DNA aptamers: A mini-review. *Journal of Molecular Graphics & Modelling*, *105*, 107872. https://doi.org/10.1016/j.jmgm.2021.107872

Alhadrami, H. A., Chinnappan, R., Eissa, S., Rahamn, A. A., & Zourob, M. (2017). High affinity truncated DNA aptamers for the development of fluorescence based progesterone biosensors. *Analytical Biochemistry*, *525*, 78–84. https://doi.org/10.1016/j.ab.2017.02.014

Aubin-Tam, M.-E., Appleyard, D. C., Ferrari, E., Garbin, V., Fadiran, O. O., Kunkel, J., & Lang, M. J. (2011). Adhesion through single peptide aptamers. *The Journal of Physical Chemistry. A*, *115*(16), 3657–3664. https://doi.org/10.1021/jp1031493

Baptista, L. A., & Netz, P. A. (2019). Single molecule force spectroscopy of a streptomycin-binding RNA aptamer: An out-of-equilibrium molecular dynamics study. *The Journal of Chemical Physics*, *151*(19), 195102.

Berendsen, H. J., Postma, Jv., van Gunsteren, W. F., DiNola, A., & Haak, J. R. (1984). Molecular dynamics with coupling to an external bath. *Journal of Chemical Physics*, *81*(8), 3684–3690. https://doi.org/10.1063/1.448118

Blank, M., & Blind, M. (2005). Aptamers as tools for target validation. *Current Opinion in Chemical Biology*, *9*(4), 336–342. https://doi.org/10.1016/j.cbpa.2005.06.011

Bock, L. C., Griffin, L. C., Latham, J. A., Vermaas, E. H., & Toole, J. J. (1992). Selection of single-stranded DNA molecules that bind and inhibit human thrombin. *Nature*, *355*(6360), 564–566. https://doi.org/10.1038/355564a0

Bunka, D. H., & Stockley, P. G. (2006). Aptamers come of age - at last. *Nature Reviews. Microbiology*, *4*(8), 588–596. https://doi.org/10.1038/nrmicro1458

Case, D. A., Belfon, K., Ben-Shalom, I., Brozell, S. R., Cerutti, D., Cheatham, T., Cruzeiro, V. W. D., Darden, T., Duke, R. E., & Giambasu, G., Amber 2020 (2020).

Case, D. A., Cheatham, T. E., III, Darden, T., Gohlke, H., Luo, R., Merz, K. M., Jr, Onufriev, A., Simmerling, C., Wang, B., & Woods, R. J. (2005). The Amber biomolecular simulation programs. *Journal of Computational Chemistry*, *26*(16), 1668–1688. https://doi.org/10.1002/jcc.20290

Chen, Z., Hu, L., Zhang, B.-T., Lu, A., Wang, Y., Yu, Y., & Zhang, G. (2021). Artificial intelligence in aptamer–target binding prediction. *International Journal of Molecular Sciences*, *22*(7), 3605. https://doi.org/10.3390/ijms22073605

Da Silva, A. W. S., & Vranken, W. F. (2012). ACPYPE-Antechamber python parser interface. *BMC Reearch Notes*, *5*, 1–8.

Darden, T., York, D., & Pedersen, L. (1993). Particle mesh Ewald: An N·log (N) method for Ewald sums in large systems. *Journal of Chemical Physics*, *98*(12), 10089–10092. https://doi.org/10.1063/1.464397

de Oliveira, R. C., Paschoal, J. A. R., Sismotto, M., da Silva Airoldi, F. P., & Reyes Reyes, F. G. (2009). Development and validation of an LC-APCI-MS-MS analytical method for the determination of streptomycin and dihydrostreptomycin residues in milk. *Journal of Chromatographic Science*, *47*(9), 756–761. https://doi.org/10.1093/chromsci/47.9.756

Dua, P., Kim, S., & Lee, D-k. (2011). Nucleic acid aptamers targeting cell-surface proteins. *Methods (San Diego, Calif.)*, *54*(2), 215–225. https://doi.org/10.1016/j.ymeth.2011.02.002

Ellington, A. D., & Szostak, J. W. (1990). In vitro selection of RNA molecules that bind specific ligands. *Nature*, *346*(6287), 818–822. https://doi.org/10.1038/346818a0

Emrani, A. S., Danesh, N. M., Lavaee, P., Ramezani, M., Abnous, K., & Taghdisi, S. M. (2016). Colorimetric and fluorescence quenching aptasensors for detection of streptomycin in blood serum and milk based on double-stranded DNA and gold nanoparticles. *Food Chemistry*, *190*, 115–121. https://doi.org/10.1016/j.foodchem.2015.05.079

Flores, S. C., Sherman, M., Bruns, C. M., Eastman, P., & Altman, R. B. (2011). Fast flexible modeling of RNA structure using internal coordinates. *IEEE/ACM Transactions on Computational Biology and Bioinformatics*, *8*(5), 1247–1257. https://doi.org/10.1109/TCBB.2010.104

Frisch, M., Trucks, G., Schlegel, H., Scuseria, G., Robb, M., Cheeseman, J., Scalmani, G., Barone, V., Mennucci, B., & Petersson, G. (2009). *GAUSSIAN09*. Gaussian Inc.

Ghanbari, K., & Roushani, M. (2018). A novel electrochemical aptasensor for highly sensitive and quantitative detection of the streptomycin antibiotic. *Bioelectrochemistry (Amsterdam, Netherlands)*, *120*, 43–48. https://doi.org/10.1016/j.bioelechem.2017.11.006

Granja, R. H., Niño, A. M. M., Zucchetti, R. A., Niño, R. E. M., Patel, R., & Salerno, A. G. (2009). Determination of streptomycin residues in honey by liquid chromatography-tandem mass spectrometry. *Analytica Chimica Acta*, *637*(1–2), 64–67. https://doi.org/10.1016/j.aca.2009.01.006

Hess, B., Bekker, H., Berendsen, H. J., & Fraaije, J. G. (1997). LINCS: a linear constraint solver for molecular simulations. *Journal of Computational Chemistry*, *18*(12), 1463–1472. https://doi.org/10.1002/(SICI)1096-987X(199709)18:12<1463::AID-JCC4>3.0.CO;2-H

Hess, B., Kutzner, C., Van Der Spoel, D., & Lindahl, E. (2008). GROMACS 4: Algorithms for highly efficient, load-balanced, and scalable molecular simulation. *Journal of Chemical Theory and Computation*, *4*(3), 435–447. https://doi.org/10.1021/ct700301q

Humphrey, W., Dalke, A., & Schulten, K. (1996). VMD: visual molecular dynamics. *Journal of Molecular Graphics*, *14*(1), 33–38. https://doi.org/10.1016/0263-7855(96)00018-5

Jayasena, S. D. (1999). Aptamers: an emerging class of molecules that rival antibodies in diagnostics. *Clinical Chemistry*, *45*(9), 1628–1650. https://doi.org/10.1093/clinchem/45.9.1628

Kaur, H., & Yung, L.-Y. L. (2012). Probing high affinity sequences of DNA aptamer against VEGF165. *PloS One*, *7*(2), e31196. https://doi.org/10.1371/journal.pone.0031196

Keefe, A. D., Pai, S., & Ellington, A. (2010). Aptamers as therapeutics. *Nature Reviews. Drug Discovery*, *9*(7), 537–550. https://doi.org/10.1038/nrd3141

Krieger, R. (2001). *Handbook of pesticide toxicology: Principles and agents*. Academic press.

Kumari, R., Kumar, R., & Lynn, A., Open Source Drug Discovery Consortium. (2014). g_mmpbsa-a GROMACS tool for high-throughput MM-PBSA calculations. *Journal of Chemical Information and Modeling*, *54*(7), 1951–1962. https://doi.org/10.1021/ci500020m

Le, T. T., Chumphukam, O., & Cass, A. E. (2014). Determination of minimal sequence for binding of an aptamer. A comparison of truncation and hybridization inhibition methods. *RSC Advances.*, *4*(88), 47227–47233. https://doi.org/10.1039/C4RA08243E

Liu, J., Cao, Z., & Lu, Y. (2009). Functional nucleic acid sensors. *Chemical Reviews*, *109*(5), 1948–1998.

Nick, T. A., de Oliveira, T. E., Pilat, D. W., Spenkuch, F., Butt, H-Jr., Helm, M., Netz, P. A., & Berger, Rd. (2016). Stability of a split streptomycin binding aptamer. *The Journal of Physical Chemistry. B*, *120*(27), 6479–6489. https://doi.org/10.1021/acs.jpcb.6b02440

Robertson, D. L., & Joyce, G. F. (1990). Selection in vitro of an RNA enzyme that specifically cleaves single-stranded DNA. *Nature*, *344*(6265), 467–468. https://doi.org/10.1038/344467a0

Roushani, M., Ghanbari, K., & Hoseini, S. J. (2018). Designing an electrochemical aptasensor based on immobilization of the aptamer onto nanocomposite for detection of the streptomycin antibiotic. *Microchemical Journal*, *141*, 96–103. https://doi.org/10.1016/j.microc.2018.05.016

Stefanucci, A., Amato, J., Brancaccio, D., Pagano, B., Randazzo, A., Santoro, F., Mayol, L., Learte-Aymamí, S., Rodriguez, J., Mascareñas, J. L., Novellino, E., Carotenuto, A., & Mollica, A. (2021). A novel β-hairpin peptide derived from the ARC repressor selectively interacts with the major groove of B-DNA. *Bioorganic Chemistry*, *112*, 104836. https://doi.org/10.1016/j.bioorg.2021.104836

Stefanucci, A., Mosquera, J., Vázquez, E., Mascareñas, J. L., Novellino, E., & Mollica, A. (2015). Synthesis, characterization, and DNA binding profile of a macrocyclic β-sheet analogue of ARC protein. *ACS Medicinal Chemistry Letters*, *6*(12), 1220–1224. https://doi.org/10.1021/acsmedchemlett.5b00363

Sussman, D., Nix, J. C., & Wilson, C. (2000). The structural basis for molecular recognition by the vitamin B 12 RNA aptamer. *Nature Structural Biology*, *7*(1), 53–57. https://doi.org/10.1038/71253

Taghdisi, S. M., Danesh, N. M., Nameghi, M. A., Ramezani, M., & Abnous, K. (2016). A label-free fluorescent aptasensor for selective and sensitive detection of streptomycin in milk and blood serum. *Food Chemistry*, *203*, 145–149. https://doi.org/10.1016/j.foodchem.2016.02.017

Tereshko, V., Skripkin, E., & Patel, D. J. (2003). Encapsulating streptomycin within a small 40-mer RNA. *Chemistry & Biology*, *10*(2), 175–187. https://doi.org/10.1016/S1074-5521(03)00024-3

Trott, O., & Olson, A. J. (2010). AutoDock Vina: Improving the speed and accuracy of docking with a new scoring function, efficient optimization, and multithreading. *Journal of Computational Chemistry*, *31*(2), 455–461. https://doi.org/10.1002/jcc.21334

Wegener, H. C. (2003). Antibiotics in animal feed and their role in resistance development. *Current Opinion in Microbiology*, *6*(5), 439–445. https://doi.org/10.1016/j.mib.2003.09.009

Winkler, W., Nahvi, A., & Breaker, R. R. (2002). Thiamine derivatives bind messenger RNAs directly to regulate bacterial gene expression. *Nature*, *419*(6910), 952–956. https://doi.org/10.1038/nature01145

Yin, J., Guo, W., Qin, X., Pei, M., Wang, L., & Ding, F. (2016a). A regular "signal attenuation" electrochemical aptasensor for highly sensitive detection of streptomycin. *New Journal of Chemistry*, *40*(11), 9711–9718. https://doi.org/10.1039/C6NJ02209J

Yin, J., Guo, W., Qin, X., Zhao, J., Pei, M., & Ding, F. (2017). A sensitive electrochemical aptasensor for highly specific detection of streptomycin based on the porous carbon nanorods and multifunctional graphene nanocomposites for signal amplification. *Sensors and Actuators B: Chemical*, *241*, 151–159. https://doi.org/10.1016/j.snb.2016.10.062

Yin, Y., Qin, X., Wang, Q., & Yin, Y. (2016b). A novel electrochemical aptasensor for sensitive detection of streptomycin based on gold nanoparticle-functionalized magnetic multi-walled carbon nanotubes and nanoporous PtTi alloy. *RSC Advances*, *6*(45), 39401–39408. https://doi.org/10.1039/C6RA02029A

Zhao, J., Wu, Y., Tao, H., Chen, H., Yang, W., & Qiu, S. (2017). Colorimetric detection of streptomycin in milk based on peroxidase-mimicking catalytic activity of gold nanoparticles. *RSC Advances*, *7*(61), 38471–38478. https://doi.org/10.1039/C7RA06434A

Zhou, N., Wang, J., Zhang, J., Li, C., Tian, Y., & Wang, J. (2013). Selection and identification of streptomycin-specific single-stranded DNA aptamers and the application in the detection of streptomycin in honey. *Talanta*, *108*, 109–116. https://doi.org/10.1016/j.talanta.2013.01.064

Zuker, M. (2003). Mfold web server for nucleic acid folding and hybridization prediction. *Nucleic Acids Research*, *31*(13), 3406–3415. https://doi.org/10.1093/nar/gkg595